Feedback controlled high frequency electrochemical micromachining

F.M. Ozkeskin[1], S.S. Sundarram[1], S. Allison[1], N.P. Hung[1], M. Powers[2], G. Strohm[3], L.A. Godinez[4], and J.R. Mariquez[4]

[1] Texas A&M University, College Station, TX, USA
[2] Agilent Technologies, Santa Rosa, CA, USA
[3] Ohio State University, Columbus, OH, USA
[4] Cideteq, Queretaro, Mexico

Keywords: Electrochemical micromachining, electrode position control, inter electrode gap.

Abstract:

The mostly used processes for microsystem and integrated circuitry components manufacturing are often leveraged from semiconductor technologies. Although popular in electronics, silicon does not have adequate properties for demanding applications in aerospace, mechanical, or biomedical. Fabrication using high strength metals, like stainless steel and superalloys, requires novel technologies which are different from those for silicon. A promising manufacturing method for mass producing of micro/meso scale components is electrochemical micromachining (microECM). No electrode wear, non contact process, no workpiece subsurface damage... are among the advantages of microECM. The complex system, however, requires high precision mechanical fixtures and sophisticated instrument for proper process control. This study presents a microECM system with dynamic closed-loop feedback control. The system, improves significantly material removal rate by optimizing inter electrode gap, reducing machining time, and producing higher quality microcomponents.

Introduction

The fabrication methodology of microsystems and integrated circuitry components is well-known and it has become practically abundant [1]. The silicon micromachining technology has been practiced in several applications extending from microelectromechanical systems (MEMS) sensors and actuators [2] to biomedical uses [3]. The semiconducting properties of silicon make it popular in electronics, but lack of mechanical properties makes silicon vulnerable to many other applications that demands high stress and temperature. Micromachining alternative engineering alloys such as stainless steel, titanium or superalloys must be done with other novel methods. An emerging technology for micro/meso scale components is the electrochemical micromachining (microECM).

MicroECM has emanated as a non-conventional micromachining technology. Among many novel machining processes [4, 5], microECM has received growing interest from industry in the last fifteen years due to its multifarious advantages which have been demonstrated in numerous applications [6-8]. MicroECM, as an anodic dissolution process with workpiece being an anode, has atomic size material removal nature which yields smoother surface finish in absence of burr. High material removal rate (MRR), no tool wear due to non-contact machining and avoidance of subsurface damage are of primary reasons to propose this technique for machining sophisticated shapes regardless of the material strength and hardness. MicroECM works with all electrochemically active materials such as metals and semiconductors [9]. It has found its place in machining a wide range of parts from large turbine blades to complex microparts [10-12].

There are many factors affecting both MRR and quality of electrochemically machined profiles [13]. The electrolyte, conventionally a concentrated salt solution, is pumped through the electrode gap to carry the electrons causing anode workpiece to dissolve regionally. It also helps carrying the reaction products away and sinking the generated heat. Concentration and flow rate studies are done and specific electrolytes for particular purposes have been characterized [14-16].

The applied voltage waveform plays a crucial role in defining a profile quality and surface finish of microECM'ed part. In the last decade, ultrashort pulse microECM has been studied [9, 17-20]. With the use of ultrahigh frequency inputs around GHz range, electrochemical reactions are restricted to electrode regions in close proximity which exceeds far beyond the 0.1mm limited spatial resolution defined solely by electrolytic current density in DC voltages [9]. This application resulted in increasing accuracy but reducing machining efficiency. The MRR, therefore, is decreased due to highly confined electron motion, eventuating a major problem in ultrashort pulsed systems [15, 21].

To invoke localized anodic dissolution, the tool electrode is brought at the proximity of workpiece electrode and the inter electrode gap (IEG) has been reduced as much as possible within the limits of actuators and measurability [22]. Specific IEG is around 10-25μm and is being reduced to sub-micron level with the use of piezo-driven stages and sub-50μm diameter cylindrical wires [9]. The MRR is relatively increased this way by providing a vertical removal giving a deeper slot or a hole. However, even a very small pattern of few microns depth can take up to several minutes to machine.

To achieve both accuracy and efficiency concurrently, larger cross section electrodes have been employed driving larger powers while keeping the IEG smaller. This approach, even though seems feasible, often generates a damaging micro-spark [23]. Higher machining voltages with high electrolyte concentration increase the speed of dissolution, developing an increase in hydrogen generation. The heated hydrogen bubbles prevent laminar electrolyte flow in a close proximity and the cavities formed in the flow along with electrolyte salt precipitation on tool cause a short circuiting ending with micro-sparks. Large surface pits are often observed. Although IEG is not intended to diminish beyond certain point, unexpected machining dynamics can cause this behavior. High tool feed rate can cause electrode contact and short circuiting [24]. However if it is too slow, the profiles will have round edge problem at the hole orifice and tapered side walls inside the hole due to excessive machining even if the tool electrode is side insulated to prevent side wall current distribution [25, 26]. The lack of accurate control at that point could end up with an undesired increase in machining time.

While no single and ultimate solution can be suggested to accuracy-efficiency dilemma in the presence of a multivariable system, a feedback control approach can reduce the machining time significantly. The tool electrode brought directly to the machining range where the current density is at maximum in a given interval and keeping it constant is essential in the increasing efficiency.

This paper presents a custom built closed-loop system in which the current flow is used as a dynamic feedback signal.

System Process Control

A high frequency closed-loop microECM system was designed. The signals acquired from an ammeter and laser displacement sensor, for current and position feedbacks respectively were evaluated on a controlling computer. The communication is provided over serial communication ports through a serial instrument controller interface board. The output signal was manipulated as per input evaluations and sent to actuators to complete the required action. The Instrument schematic is illustrated in Fig. 1.

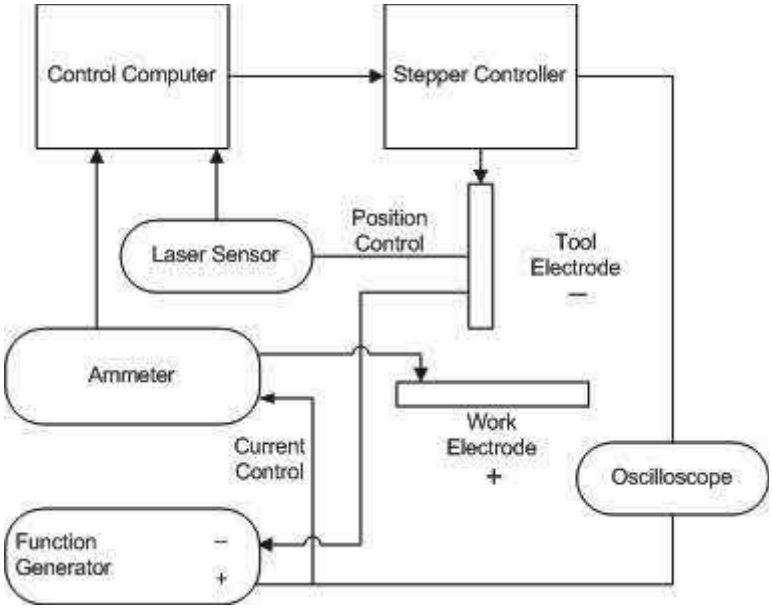

Fig. 1. Current and position controlled setup.

The current density-IEG relation can be summarized combining Tafel's equation and Ohm's Law (1). The MRR is obtained using Faraday's law (2).

$$j = j_0 e^{\alpha\eta\frac{\varepsilon}{kT}} = \frac{E(t)}{gr} \quad , \tag{1}$$

$$V = \int_0^{\tau} \frac{CEAdt}{gr} \quad , \tag{2}$$

Where,

j: dissolution current density (A/m^2),
α: charge transfer coefficient,
ε: elementary electric charge (C),
T: electrolyte temperature (ºK),
g: the electrode workpiece gap or IEG (m),
V: removal volume (m^3),
C: specific removal rate (mm^3/A-s),
j_0 : exchange current density at equilibrium (A/m^2),
η: overpotential (V),
k: Boltzmann constant,
$E(t)$: applied voltage (V),
r: electrolyte resistivity (Ωm),
τ: pulse duration (s),
A: surface area of tool (m^2).

Equation (1) states the inversely proportional linear relation of IEG and current density. Decreasing electrode gap causes an increase in the output current density; the current change would provide informative data of the electrode position.

For closed-loop experiments, binary logic control algorithm was written in Labview version 8.2. The control logic data flow is depicted in Fig. 2. For the sake of simplicity manual start and stop buttons are omitted in depiction even though they are functional. There are two control loops in the program algorithm; in the first loop, displacement sensor output data is checked to see if the tool is in active machining zone or not. If the laser is in reading range, the program starts and current value is recorded. If not, the tool electrode is fast forwarded to the reading range. When the tool reached the desired final depth, the system terminates actuation and pulls the tip back to initial home position.

In the second loop, the current values dictate subsequent action. Limit set conditions are determined by the preliminary experiments for calibration purposes, yielding a stable machining current interval. If the present current reading is below the lower value, it is interpreted that the tool is not in machining zone yet; consequently the stepper motor carrying the tool is driven forward in a user defined pace. If the recorded data is between upper and lower current reading intervals, system stands by and machining continues. If it is beyond the upper limit, then a fast backward pulling action is executed to separate the tools.

Velocity control is achieved using a similar approach. A current jump beyond the expected linear region on the current output data however still below the upper limit indicates the tool electrode approaching to the workpiece electrode fast. The z-directional feed rate is reduced by half for the rest of the operation to avoid a short-circuit. Also, given the possibility of starting the program on a random height beyond the reading range of laser sensor, the electrode has been driven in a fast speed determined by user inputted proportional constant until first reading from the laser is recorded.

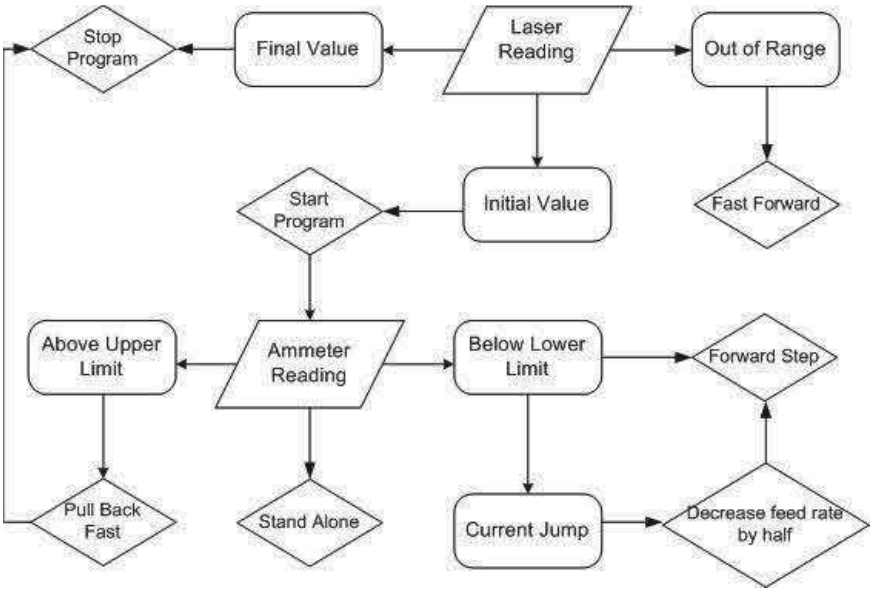

Fig. 2. Flow chart of tool electrode position and velocity control.

Experimental Procedure

A closed-loop microECM system was developed in our laboratory (Fig. 3). A bidirectional manipulator using stepper motors with 2.5µm step size and 250mm travel distance (VXM, Velmex, Inc.) was used as actuator mechanism. A 316L stainless steel pin, Ø 500µm, with ground and polished flat end, was rigidly clamped into a tool holder.

Environmentally friendly $NaNO_3$ electrolyte was preferred over acidic solutions [11, 12]. The concentration was kept at 30g/l. The electrolyte was pumped and submerged tool electrode in a columnar flow.

The workpiece material was 0.5mm-thick 316L stainless steel plate. A function generator (CFG250, Tektronix, Inc.) supplied the system with pulsed square wave in the range of 0.5-50 KHz. A digital oscilloscope (TDS 1002B, Tektronix, Inc.) provided online signal evaluation and an ammeter (Model 45, Fluke Electronics) was used to monitor current change in the cell for feedback signal. A 0.1µm resolution laser displacement sensor (LK-G157, Keyence) was utilized to measure the displacement between the tool electrode workpiece. All the communications were provided using a serial communication board (PCI-8432/4, National Instruments).

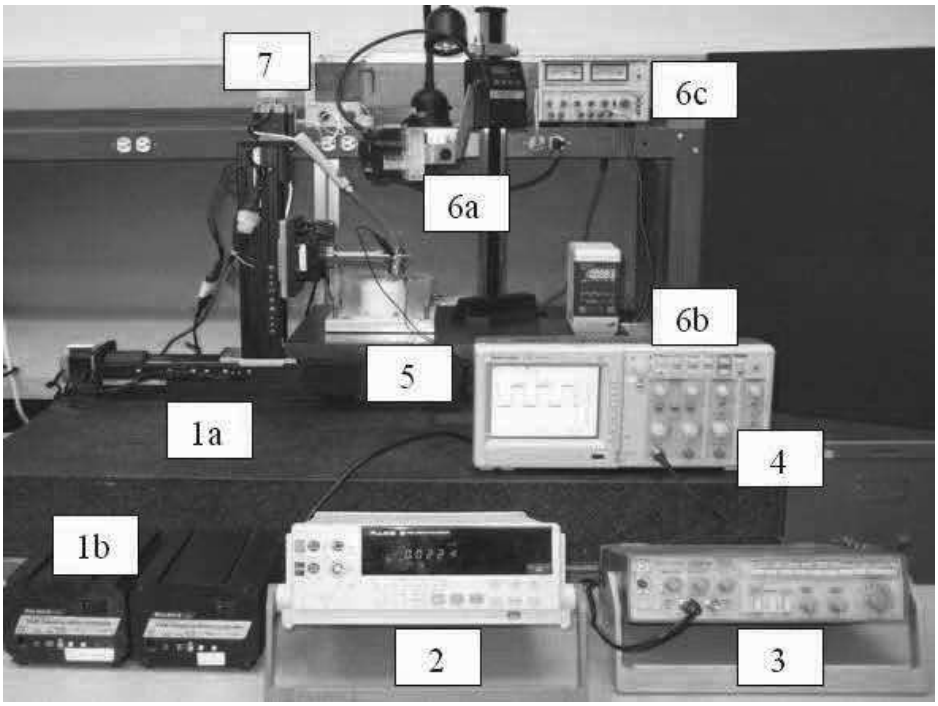

Fig. 3. Closed-loop microECM setup. (1a) stepper motors, (1b) motor controller, (2) ammeter, (3) function generator, (4) oscilloscope, (5) ECM cell, (6a) laser displacement sensor, (6b) laser controller and display, (6c) power source for laser unit, (7) electrolyte tank and jet pump.

Open-loop experiments were first tested by giving constant feed rate and displacement commands to stepper motor controllers. Machined features were measured with an optical measuring microscope (STM6, Olympus, 0.1 μm resolution). The material removal rate was calculated from removed weight over time and measured with a high precision weight balance (LE26P, Sartorius, 1μg resolution).

Closed-loop experiments were carried out in a parametric method. The pulsed voltage amplitude was 16 V peak-to-peak with a minimum of -4V and a maximum of 12V for all experiments. The relatively small inverse polarity was required to promote the possible dissolution of plated product on the tool electrode during an inverse pulse [27, 28]. The pulse-on and pulse-off time ratio was kept at 2:1, which was long enough to dissipate heated electrolyte and produced gas. All open loop experiments were run at a motor speed of 5mm/sec.

Hole depths and diameters were measured after 60 seconds. A total of 70 holes were machined with 7 different frequencies, 5 repeats on both closed and open-loop systems. Same profiles were quantified for depth, diameter and MRR.

A separate set of experiments were realized for system hysteresis behavior. The depths were programmed to be 25μm, 50μm, 100μm and 200μm in forward and backward directions to note any hyterical variations. The experiments were repeated twice for both 500 Hz and 50 KHz frequencies.

Results and Discussion

Initial open-loop run was necessary to calibrate the current-IEG relationship (Fig. 4). Current values were normalized to current densities by including area of tool electrode. Drastic drop of current density was seen at IEG about 20µm. Therefore, the machining current density limits were determined to be on an effective range from 300mA/mm^2 to 350mA/mm^2. The control algorithm upper and lower limits were set to be on this range.

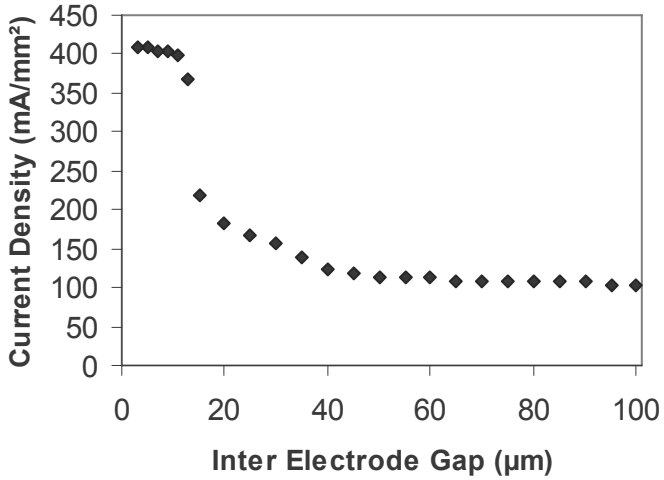

Fig. 4. Effect of electrode gap on ECM current density. 30 g/L $NaNO_3$, 500 Hz, 16V pp.

Effect of Frequency on the Hole Depth and Diameter

Hole diameter and hole depth versus frequency are plotted in Fig. 5. Quantitative decrease in the both features is noticed with increasing frequency. It is observed that open-loop system creates bigger hole openings on the surface since there was an uncertain time spent in between machining steps using constant velocity, bringing an undesired size increase on the orifice and introduce a non-uniform hole profile along the depth. The uncertainty can also be seen by noticing on the size variations. On the other hand the closed-loop system is remarkably better in achieving deeper profiles. The controlled tool speed and displacement increased the efficiency in reaching much higher aspect ratios when combined with the smaller diameter holes. The closed-loop system has proven to be repeatable and it is seen in low variation values on plots.

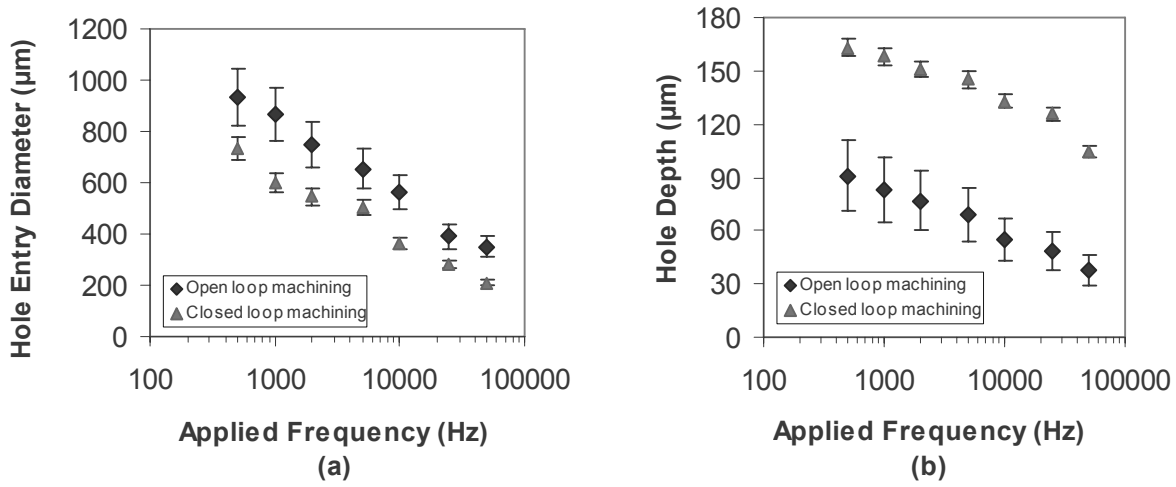

Fig. 5. Effect of frequency on (a) diameters and (b) depths for open and closed-loop machining. 30 g/L $NaNO_3$, 500 Hz, 16V pp, Ø 0.5mm tool electrode.

Effect of Frequency on MRR

Figure 6 shows the MRR by theory and experiments. The theoretical value of removal volume is calculated using equation (2). Feedback controlled closed-loop system had a significant advantage due to the deeper hole profiles and less amount of machining time spent as a result of both velocity and displacement control. Closed-loop machining MRR converged to the theoretical values by an increase of 250% on open-loop machining. The repeatability was most obvious in MRR experiments since even a small time loss has a dramatic effect on a relatively short machining time of one minute. The average variation in MRR was reduced by 88% in closed-loop machining.

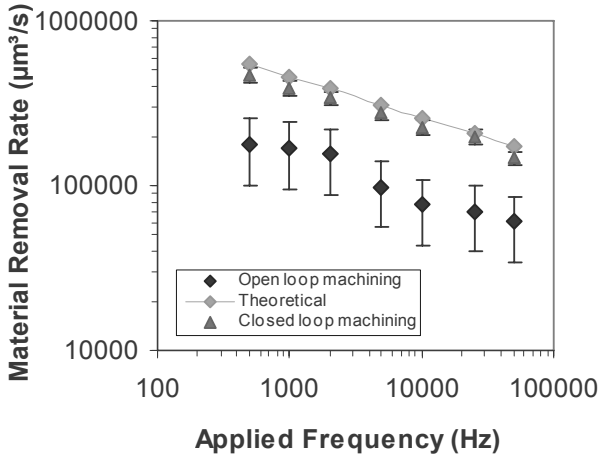

Fig. 6. Material removal rate with frequency. 30 g/L $NaNO_3$, 500 Hz, 16V pp, Ø 0.5mm tool electrode.

Hole Profile

By utilizing the closed-loop control, we investigated the entry/exit hole uniformity, variations and enhancements over open-loop system by drilling through holes. The resulting optical images are given in Fig. 7. The exit holes were all same for both open and closed-loop control systems. The open-loop entry hole had a large bowl like shape and a very large initial diameter due to already explained reasons, whereas closed-loop entry hole shape was more resembling to exit hole, having sharper edges with smaller curvature radius. The open-loop hole profiles were overall bigger in diameter as a non-uniform machining routine is followed throughout machining. Undesired surface damage decreased 97% due to closed-loop controlled machining.

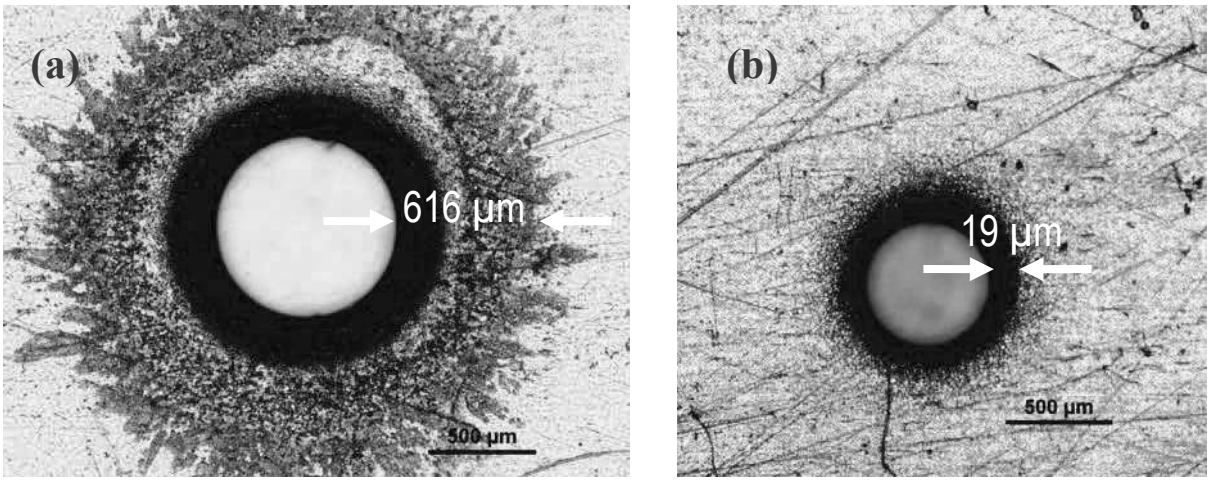

Fig. 7. MicroECM hole profile images. Top view of entry hole after ECM'ing with (a) open loop control and (b) closed-loop control.

System Hysteresis

The hysteresis on programmed and measured hole depths is shown in Fig. 8. No hysteresis was observed and high conciliation of programmed and measured hole depth was established at both low and high frequencies.

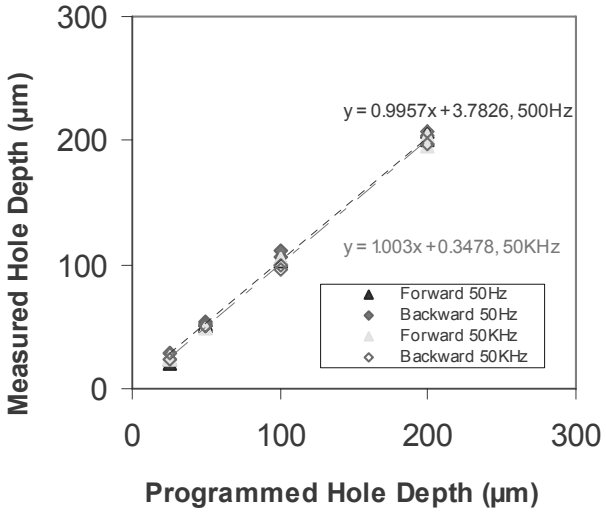

Fig. 8. 500 Hz and 50 Khz hysteresis study.

Conclusion and Recommendation

A microECM system with closed-loop control was developed. It was found that high frequency pulsed input reduced feature size and material removal rate but improved feature quality. Binary algorithms were applied to certain machining scenarios to take measures and manipulate output. Closed-loop inter electrode gap control provides faster machining time and higher material removal rate.

The system can be further improved by providing real time control of pulse amplitude from the power supply in addition to current control.

Acknowledgement

This study is generously supported by TAMU-CONACyT and Agilent Technologies.

References

1. Rai-Coudhury P., Ed., Handbook of *Microlithography, Micromachining & Microfabrication* SPIE Optical Engineering Press, Bellingham, WA (1997).

2. Jerman H., Terry S., *Microlithography, Micromachining & Microfabrication,* vol. 2, pp.379-434 SPIE Optical Engineering Press, Bellingham, WA (1997).

3. Santini, J. T., Cima, M. J., Langer, R., *Nature* **397**, 335 (1999).

4. Wilson, J. F., *Practical and Theory of Electrochemical Machining*, Wiley Interscience, New York, NY, USA (1971).

5. Mishra, P.K., *Non-Conventional Machining*, Narosa Publishing House, New Delhi, India (1997).

6. Datta, M., *Electrochemical Micromachining*. In: Masuko, M., Osaka, T. and Ito, Y., Editors, Electrochemical Technology: Innovation and New developments, Dordon and Breach Science Publishers, pp. 137-157, Tokyo (1996).

7. Datta, M., Harris, H., *Electrochimica Acta* **42**, 3007 (1997).

8. Datta, M., *IBM Journal of Research and Development* **42**, 655 (1998).

9. Schuster, R., Kircher, V., Allongue, P., Ertl, G., *Science* **289**, 98 (2000).

10. Datta, M., Shenoy, R.V., Rominkiw, L.T., *Transactions of the ASME* **118**, 29 (1996).

11. Osenbrugger, C., Regt, C. *Philips Technical Review* **42**, 22 (1985).

12. Datta, M., Romankiw, L.T., *Journal of the Electrochemical Society* **136**, 285 (1989).

13. Tenigyahi, N., *Annals of the CIRP* **32**, 573 (1983).

14. Dabrowski, L., Paczkowski, T., *Russian Journal of Electrochemistry* **41**, 91 (2005).

15. Davydov, A.D., Volgin, V.M., Lyubimov, V.V., *Russian Journal of Electrochemistry* **40**, 1230 (2004).

16. Jain, V.K., Rajurkar, K.P., *Precision Engineering* **13**, 111 (1991).

17. Amalnik, M.S., McGeough, J.A., *Journal of Material Processing Technology* **61**, 139 (1996).

18. Bhattacharyya, B., Munda, J., *International Journal of Machine Tools and Manufacture* **43**, 1301 (2003).

19. Kozak, J., Rajurkar K.P, Wei, B., *Transactions of the ASME* **116**, 316 (1994).

20. Maeda, R., Chikamori, K., *Yamamoto, H., Precision Engineering* **6**, 193 (1984).

21. Kenney, A. J., Hwang, S. Gyeong., *Nanotechnology* **16**, 309 (2005).

22. Rajurkar, K.P., Zhu, D., McGeough, J.A., Kozak, J., De Silva, A., *Annals of the CIRP*

48, 567 (1999).

23. Lu, X., Leng, Y., *Journal of Materials Processing Technology* **169**, 173 (2005).

24. Bhattacharyya, B., Malapati, M., Munda, J., *Journal of Materials Processing Technology* **169**, 485 (2005).

25. Yong, L., Yunfei, Z., Guang, Y., Liangqiang, P., *Sensors and Actuators A* **108**, 144 (2003).

26. Ahn, S. H., Ryu, S. H., Choi, D.K., Chu, C.N., *Precision Engineering* **28**, 129 (2004).

27. Zhou, C.D., Taylor, E.J., Sun, J.J., Gebralt, L., Stortz, E.C., Renz, R.P., *Transactions NAMRI/SME* **25**, 147 (1997).

28. Uhlmann, E., Doll, U., Forster, R., Schikofsky, R., *Proceedings International Symposium for Electromachining (ISEM XIII)*, 261, Bilbao (2001).

Author Biography

Fatih Mert Ozkeskin received his B.S. degree on Mechatronics Engineering at Sabanci University, Turkey. He is currently a graduate student in Mechanical Engineering Department at Texas A&M University, College Station, USA. His research interests are applying control system to micro-meso scale applications, electrochemical micromachining and industrial robotics.